

Periodic Crazeing on Polymethylmethacrylate Film by Localized Bending

Keishi Naito, Akiyoshi Takeno, Minoru Miwa

Department of Materials Science and Technology, Faculty of Engineering, Gifu University, Gifu-shi, Gifu 501-1193, Japan

Correspondence to: K. Naito (E-mail: p3813001@edu.gifu-u.ac.jp)

ABSTRACT: Crazeing was induced on a polymethylmethacrylate film using an original, low-cost, simple process in which the film was bent using a wedge-shaped plate (referred to herein as a crazeing edge, or an edge). In this process, stress concentration and stress opening occur spontaneously by feeding the film past the edge, and crazeing is periodically induced (periodic craze). The craze interval, width, and depth depend on the localized bending conditions at the tip of the edge. Two different types of crazeing mechanism were suggested. It was assumed that the films were either crazeed by bending along the tip of the edge or by bending according to the curvature induced by the three-point bending system. The calculated maximum stress determined by the three-point bending process and the experimental values of the craze interval and width showed similar tendencies. These results suggested that the craze depth could be determined using this bending process and known mechanical properties and crazeing conditions. © 2012 Wiley Periodicals, Inc. *J. Appl. Polym. Sci.* 000: 000–000, 2012

KEYWORDS: crazeing; processing; films; stress; morphology

Received 21 April 2011; accepted 24 March 2012; published online

DOI: 10.1002/app.37805

INTRODUCTION

If excessive force is applied to a plastic material or if a plastic film is creased, the color of the section, where the force acts or where a crease appears, may become white. In such cases, the most common reason for this color change is the generation of cracks or crazes.^{1–3} This crazeing phenomenon shows that the material is in a state of initial fracture, and this phenomenon has been widely studied as it affects the quality of films.^{4–6} The craze occurs accidentally, and usually, its occurrence greatly reduces the commercial value of the plastic products. In this study, we intentionally form craze layers at constant intervals (called periodic crazes) in polymer films using a low-cost, simple, and original process. A periodically crazeed film has been applied to films that show dynamic anisotropy or optical anisotropy and films that permeate a gas or liquid.^{7–10} The film on which the periodic craze layer was grown in the direction of the film thickness showed light-scattering characteristics, as shown in Figure 1 (when the film was observed from the front, it was transparent. However, when the film was observed from a diagonal direction, it was opaque). This viewing angle-selective film is expected to be applied in conditions where the viewing angle is limited. (e.g., information display terminal). A periodic crazeed film that is appropriate for controlling visible light, that is, as a polarizing film, has not yet been developed. It is necessary to determine the stress applied to the film when a craze is

generated and grown, and to be able to control the craze periodicity accurately. In this article, periodic crazes were induced on polymethylmethacrylate (PMMA) films. The shape of the bend at tip of the edge during periodic crazeing and the stress associated with the generation and growth of the crazeed regions were estimated.

EXPERIMENTAL

Samples

PMMA films used in this article were prepared using the cast process. Thus, the solution that PMMA particles (Mitsubishi Rayon) were stirred in a chloroform solution of 5 wt % using a magnetic stirrer for 1 day at room temperature (RT) was casted. The thickness of the films was 20–30 μm . Table I summarizes the mechanical characteristics of the PMMA films. Mechanical characteristics of PMMA films were calculated from the results of the tensile test using a tensile tester (Toyo Baldwin Tensilon-UTM-4-200). The tensile test specimen was rectangular and had a length of 50 mm and a width of 10 mm. The test conditions were as follows: gauge length, 30 mm; tensile speed, 10 mm/min; temperature, RT. The plateau modulus of the PMMA films was determined by a dynamic mechanical analysis (DMA) (TA Instrument DMA2980). The DMA sample was rectangular and had a length of 32 mm and a width of 8 mm. The measured temperature was increased from RT to 200°C, the frequency

© 2012 Wiley Periodicals, Inc.

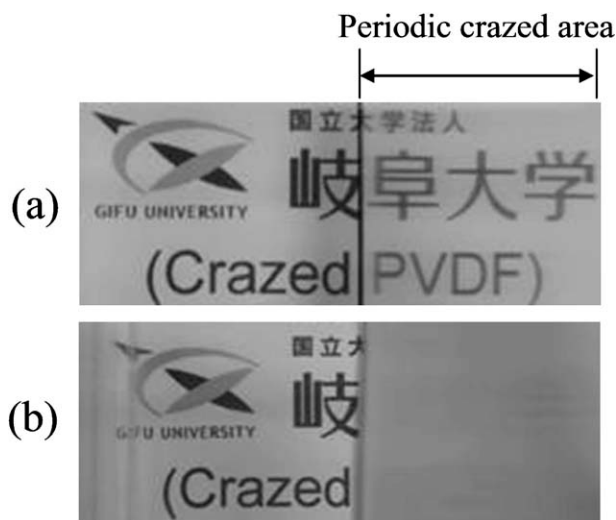


Figure 1. View point selectivity of periodically crazed films. (a) The film was parallel to the background. (b) The film was rotated with respect to the background.

was set to 10 Hz, and the deformation applied to the specimen was in the Tension Film mode. The density was measured using the Archimedes principle. Solvents used for the measurement were distilled water and ethanol, and their densities were measured using an electronic balance, used specifically to measure solid density/specific gravity (METTLER TOLEDO METTLER AT261 DeltaRange). The weight average molecular weight measured by gel permeation chromatography (GPC) was 1,440,000. The GPC measurement device consisted of a packed column (Tosoh TSK-GEL-H) for high-speed GPC, a refractive index detector, a light-scattering detector, and a differential pressure viscosity detector (Viscotek MODEL301TDA), for an organic solvent system. Standard polystyrene obtained from Viscotek was used as a standard sample for determining the calibration curve.

Crazing Process

The craze was either induced by a mechanical load or by using a solvent. The craze was induced by mechanical load grows normal to the loading direction. The solvent-induced craze occurs when the polymer is soaked in a poor solvent and then grows in the direction of the molecular orientation.^{11–13} In this article, crazing was induced in PMMA films using an original mechanical method (crazing process).

The crazing process is a simple method resulting from the bending of the material. The craze is induced periodically as the stress concentration and stress opening are spontaneous. The

Table I. Mechanical Characteristics of PMMA Films

Mechanical characteristics	PMMA
Density (g/cm ³)	1.25
Young's modulus (GPa)	1.56
Breaking strength (MPa)	50.0
Breaking strain (%)	4.49
Plateau modulus (MPa)	1620

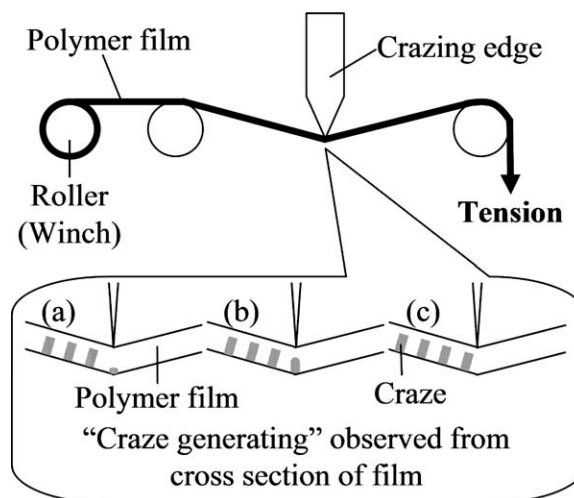


Figure 2. Schematic diagram of the crazing process. The crazing device consists of a film feed system, a tension control part, and a local bend processing part. (a) The craze is induced owing to stress concentration at the tip of the edge. (b) The Young's modulus of the section of the film where the craze is induced decreases. (c) Further crazing is not induced until the section, where a craze has been induced, moves away from the tip of the edge.

periodicity and morphology of the craze depend on the properties of the polymer film or the processing conditions.¹⁴

Figure 2 shows the crazing device. This device consists of a film feed system, a tension control part, and a local bend processing part. The film is fed through the device under constant tension (initial tension). The film is bent locally using a wedge-shaped plate (referred to as the “crazing edge” in Figure 2) and the processing angle can be varied by changing the position of the edge (vertical direction in the figure). The side which does not touch the edge in the bend section, the tension resulting from the bending is added to the initial tension applied to the film. The total tension is set higher than the stress required for craze generation and the crazing process is carried out. Crazes result from stress concentration at the tip of the edge [Figure 2(a)]. The bending tension greatly decreases owing to the decrease in the Young's modulus of the section where crazing is induced [Figure 2(b)]. Consequently, the maximum tension applied to the film decreases below that required to induce the craze-generating stress as soon as the craze is generated. As a result, further crazing is not induced until the section where the craze was induced feeds away from the tip of the edge and that the stress concentration in the film increases [Figure 2(c)]. Therefore, the craze does not grow into a crack, and the crazing process is repeated. This composite morphology can be controlled by regulating the feed rate of the film, the initial tension, and the bend tension.⁹ The crazing process was carried out under the following conditions: the processing temperature was RT, the processing angle was varied from 90 to 140°, and the processing rate was 10 mm/min.

Evaluation of Periodic Crazed Films

The morphology of the periodically crazed films was evaluated using an optical microscope (Nikon Measuring Microscope MM-400) and a scanning electron microscope (SEM, Hitachi

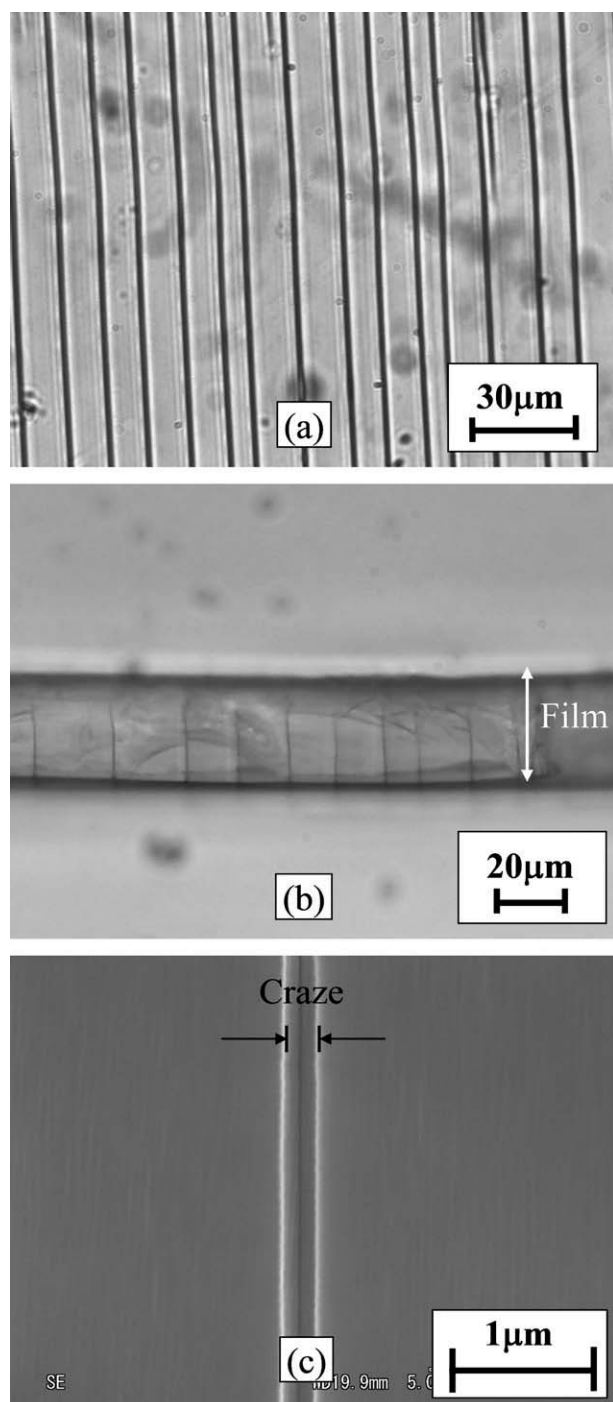


Figure 3. Images of periodically crazed PMMA films ($t = 25 \mu\text{m}$, processing stress: 13 MPa). (a) Surface and (b) cross-sectional images using an optical microscope, and (c) surface image using SEM.

PC-SEM S4300). As the sample is an insulator, it was coated with a thin layer of Pt/Pd to facilitate its observation by SEM.

RESULTS AND DISCUSSION

Periodic Crazed PMMA Films

Noncraze and craze regions are repeated at intervals of tens of micrometers during the crazing process. The generation of these

regions depends on the difference in the higher-order structure of the polymer film. Figure 3 shows an optical microscope image and a SEM image of a periodically crazed PMMA film. Figure 3(a,c) shows images of the film surface. The horizontal direction in this image is the direction in which the film was fed into the crazing device. In Figure 3(a), the vertical black stripes are the craze layers; these layers appear black because the light is scattered. Although the crazing does not appear to be periodic in the image, the periodicity can be evaluated from the craze interval determined from the image. In Figure 3(c), the white lines, in the central part of the image, indicate the limits of the craze layer. Therefore, the distance between these white lines represents the craze width. For a processing angle, processing stress and processing rate of 110° , 13 MPa, and 10 mm/min, respectively, the craze interval was $10.6 \mu\text{m}$ and the variance of craze interval was $5.0 \mu\text{m}^2$.

Figure 3(b) shows an image of the cross-section of the film where the craze grew in the depth direction. Figure 4 shows a schematic diagram of the morphology of a periodic crazed film. As shown in Figure 4, when the film was observed in the direction of the film thickness, the film had a structure in which craze layers and noncraze layers were stacked alternately.

The width of the noncraze region is referred to as the craze interval and is measured from the images obtained using the optical microscope (transmitted light mode). The width of the craze region is the craze width and is measured from the images obtained using SEM. Figure 5 shows the processing stress dependence of the craze interval and the craze width. The craze interval narrows as the processing stress increases. The variation in the craze interval decreases as the processing stress increases [Figure 5(a)]. The craze width increases with the processing stress. The variation in the craze width decreases as the processing stress increases [Figure 5(b)]. The craze depth was defined as a ratio of the length of the craze that grows in the direction of the film thickness to the overall film thickness, and was measured from the observations made using the optical microscope (transmitted light mode). The results are shown in Figure 6. The craze depth increased with the processing stress. The variation in the craze depth decreases as the processing stress increases. It is necessary to know the maximum stress that can be applied to the film to confirm the previously mentioned

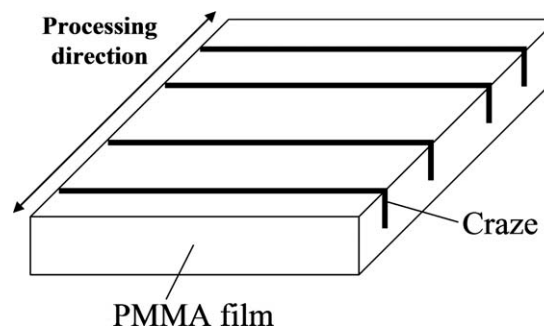


Figure 4. Schematic diagram of the morphology of a periodically crazed film.

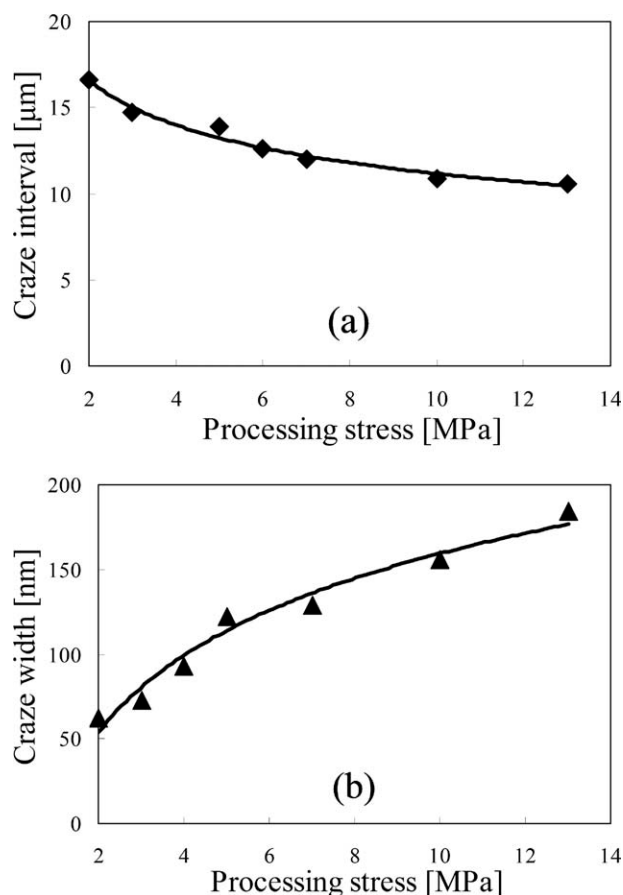


Figure 5. (a) Craze interval and (b) craze width of periodically crazed PMMA films depending on the processing stress (processing angle: 110° , processing rate: 10 mm/min).

tendency. The maximum stress is studied in the subsequent subsection.

Craze-Generating Stress

Crazing is generated at the point where the maximum stress exceeds the craze-generating stress.^{15,16} Therefore, the craze-generating stress is an important factor for determining the maximum stress that is applied to a film when craze is generated and grown. The entanglement molecular weight and the entanglement density were calculated from eqs. (1) and (2) and from the values of the density and plateau modulus of the sample film measured herein (Table I). The entanglement molecular weight was measured to be 8360 g/mol and the entanglement density was measured to be 0.150 mmol/cm³. The craze-generating stress is proportional to the square root of the entanglement density according to Wu.¹⁶ Equation (3) gives the relationship between the craze-generating stress and the entanglement density, as given by Wu. The craze-generating stress of the sample film calculated using eq. (3) was 24.4 MPa. The reported values (in the melted state, Wu^{16,17}) of the entanglement molecular weight and the craze-generating stress are 9200 g/mol and approximately 30 MPa, respectively, which do not correspond with those obtained in our study. Therefore, these values of the film which was used in our study were used

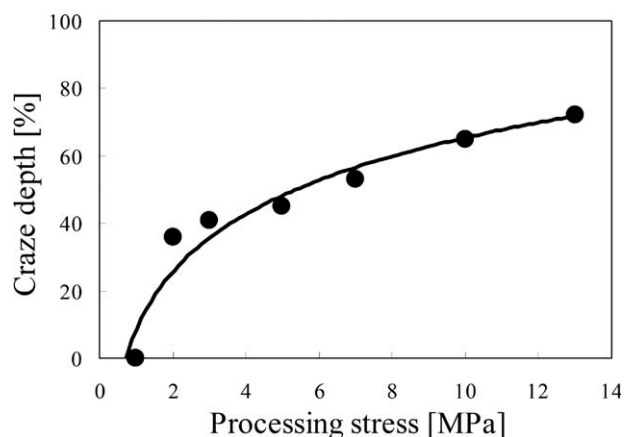


Figure 6. Craze depth of periodically crazed PMMA films depending on the processing stress (processing angle: 110° , processing rate: 10 mm/min).

in this article. The plateau modulus of the sample was measured using a DMA. The film was heated above RT and the plateau modulus was measured immediately after the temperature exceeded the glass transition temperature. The entanglement molecular weight and the entanglement density were calculated from the plateau modulus values. The results are summarized in Table II.

$$M_e = \frac{\rho RT}{E_N^0} \quad (1)$$

$$v_e = \frac{\rho}{M_e} \quad (2)$$

$$\sigma_c \propto v_e^{0.5} (\log_{10} \sigma_c \doteq \log_{10} v_e^{0.5} + 1.8) \quad (3)$$

where ρ , density (g/cm³); R , gas constant (J/K mol); T , temperature (K); E_N^0 , plateau modulus (Pa); M_e , entanglement molecular weight (g/mol); v_e , entanglement density (mol/cm³); σ_c , craze-generating stress (Pa).

Evaluation of the Maximum Stress Applied to Films

As previously stated, crazing is induced owing to the stress induced by local bending. However, the value of the bending (curvature) radius is unclear. The curvature radius of the edge of the crazing device is of the order of a few micrometers though the edge is very sharp macroscopically. Therefore, in this section, we hypothesize two theories (Figure 7) through which the maximum stress is determined. In hypothesis 1, the film bends along the shape of the tip of the edge. In hypothesis

Table II. Entanglement Molecular Weight and Craze-Generating Stress for PMMA Films^a

	ρ (g/cm ³)	M_e (g/mol)	v_e (mmol/cm ³)	σ_c (MPa)
Reference	1.17	9200	0.127	30
Experiment	1.25	8360	0.150	24.4

^a ρ , M_e , v_e , and σ_c are the density, entanglement molecular weight, entanglement density, and craze-generating stress, respectively.

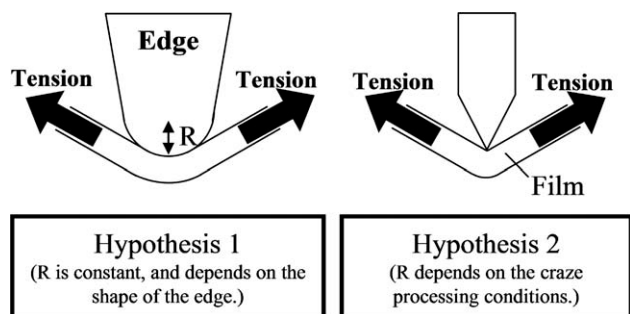


Figure 7. Pattern diagrams of the crazing process at the tip of the crazing edge according to hypothesis 1 (left) and hypothesis 2 (right).

2, the film does not bend in such a manner, and the curvature depends on the processing conditions. The suitable hypothesis is chosen based on a comparison with the experimental results.

In the case of hypothesis 1, the maximum stress is the sum of the bending stress from the edge and the processing stress (tensile stress). In hypothesis 2, it is considered that the film is a linear elastic body and that the force applied to the film is resolved into two components: the vertical component and the horizontal component. The horizontal component is the tension applied to the film (linear elastic body) [Figure 8(a,b)]. The vertical component becomes the applied force (load point) at the three-point bending of the film [Figure 8(c)]. The curvature is induced by the three-point bending [Figure 8(d)]. Though the exact shape of the bend at the tip of the edge is unclear, it may be assumed parabolic, with a variable curvature radius. The curvature radius gradually decreases as the film approaches the support point and reaches a maximum at the load point. Therefore, it is difficult to determine the shape and curvature radius. In this article, the curvature radius is calculated in a reverse manner from the experimental results for the craze depth where maximum stress is assumed. The calculation method used is as follows.

$$\sigma_{t1} = \frac{T}{bh} \quad \sigma_{t2} = \frac{T \sin(\theta/2)}{bh} \quad (4)$$

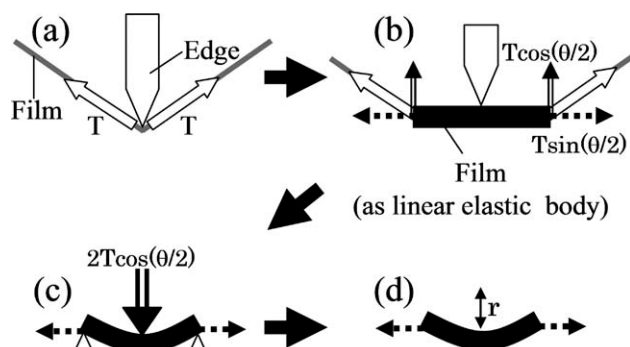


Figure 8. Pattern diagrams of the crazing process according to hypothesis 2. (a) The film is bent by the tip under a constant tension. (b) The film is assumed to be a linear elastic body and the force applied to the film is resolved into vertical and horizontal components. (c) The vertical component becomes the applied force (load point) of the three-point bending of the film. (d) The curvature is determined by the three-point bending.

Table III. Experimental and Calculated Values of the Craze Depth, Following Hypothesis 2^a

Processing stress (MPa)	Craze depth		Maximum stress (MPa)	Radius (μm)
	Experimental value (%)	Calculated value (%)		
1.0	0	0	24.4	826
2.0	25.6	23.4	31.4	656
3.0	35.7	32.6	35.0	599
5.0	48.3	43.6	40.1	541
7.0	56.6	51.4	44.1	508
10.0	65.4	59.2	47.9	491
13.0	72.0	65.1	50.0	485

^aA processing stress of 13 MPa corresponds to a breaking stress (50.0 MPa) for the PMMA films. Therefore, the maximum stress is applied to PMMA films is 50.0 MPa when the processing stress is 13.0 MPa. Calculated values of craze depth, maximum stress, and radius obtained using eqs. (4)–(7) on the basis of experimental values at a processing stress of 13.0 MPa.

$$\sigma_{b1} = \frac{Et}{R} \quad \sigma_{b2} = \frac{Et}{r} \quad (5)$$

$$\sigma_{\max 1} = \sigma_{t1} + \sigma_{b1} \quad \sigma_{\max 2} = \sigma_{t2} + \sigma_{b2} \quad (6)$$

where b , width (m); h : thickness (m); T , processing tension (N); θ , processing angle ($^\circ$); E , young's modulus (Pa); t , distance from the neutral surface to the surface (m); R , curvature radius in hypothesis 1 (m) (Constant); r , curvature radius in hypothesis 2 (m) (depends on the processing conditions); σ_{t1} , σ_{t2} , Tensile stresses in hypotheses 1 and 2, respectively (Pa); σ_{b1} , σ_{b2} , bending stresses in hypotheses 1 and 2, respectively (Pa); $\sigma_{\max 1}$, $\sigma_{\max 2}$, maximum stresses in hypotheses 1 and 2, respectively (Pa).

We hypothesized that craze growth in the direction of depth was owing to the plastic hinge principle. Rotation is advanced without the increase of the load after the bending moment became equal to the full plastic moment. The curvature is constant because the bending moment is constant. The craze layer is assumed to not contribute to the support of the beam (the film is as a linear elastic body). The maximum stress increases as t , introduced in eq. (5), decreases. This process is repeated until the maximum stress decreases below the craze-generating stress and crazing stops.

$$t_{c1} = \frac{R}{E}(\sigma_{t1} - \sigma_c) \quad t_{c2} = \frac{r}{E}(\sigma_{t2} - \sigma_c) \quad (7)$$

σ_c , craze-generating stress (Pa); t_{c1} , t_{c2} , craze depths in hypotheses 1 and 2, respectively (m).

Films used in this experiment broke at processing stresses >13.0 MPa. However, the friction between the edge and the film is applied to the film. It is necessary to consider the elastic deformation of the film from the digging action to which the film is subjected. Therefore, a processing stress of 13 MPa is equivalent to the breaking stress (50.0 MPa) for the sample film, and this value of the processing stress is normalized. In the case of

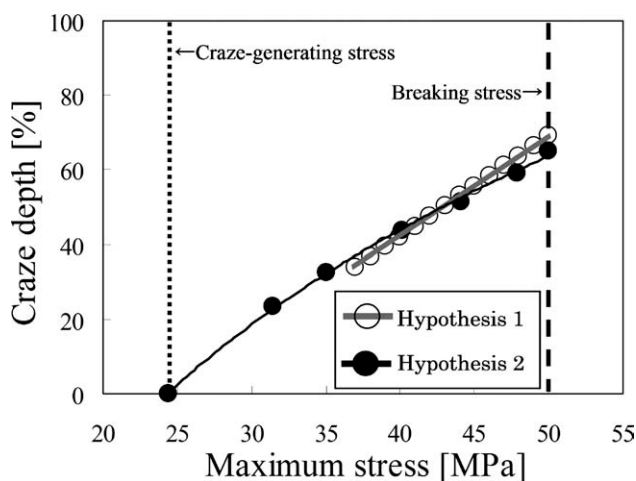


Figure 9. Maximum stress dependence vs. craze depth in PMMA films. Hypothesis 1 is shown by \circ , and hypothesis 2 is shown by \bullet (craze-generating stress: 24.4 MPa, breaking stress: 50.0 MPa).

hypothesis 1, the bending stress was $50.0 - 13.0 = 37.0$ MPa and the curvature radius can be calculated from the stress value. From the experimental results for the craze depth (Figure 6), it was observed that approximately, a 1 MPa-processing stress corresponds to the craze-generating stress, as crazing begins at this processing stress. From the craze-depth approximation, the craze reaches 65.4% of the thickness of the sample film at a processing stress of 10.0 MPa and 72.0% of the thickness of the sample film at 13.0 MPa. If the craze depth at 13.0 MPa is considered equals to 1.00, the craze depth at 10.0 MPa becomes 0.91. The calculated value of the craze depth at 13.0 MPa is 65.1% of the film thickness. Similarly, in the case of hypotheses 2, if the craze depth at 13.0 MPa is considered equals to 1.00, the craze depth at 10.0 MPa is $65.1 \times 0.91 = 59.2\%$ of the film thickness. At this craze depth, the curvature radius and the maximum stress were 491 μm and 47.9 MPa, respectively. The curvature radius and the maximum stress corresponding to the

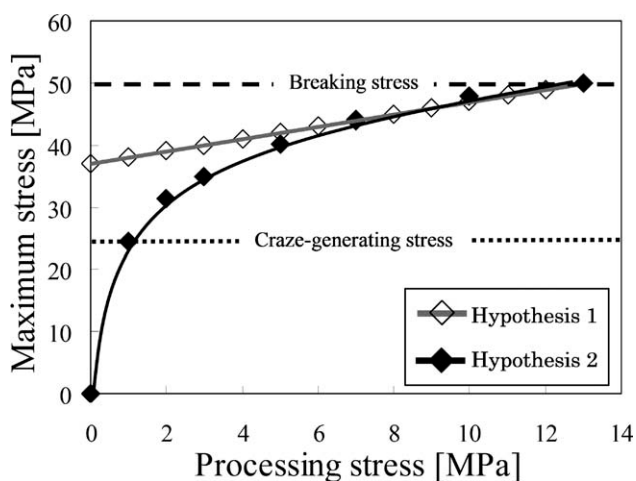


Figure 10. Processing stress dependence on maximum stress. Hypothesis 1 is shown by \diamond , and hypothesis 2 is shown by \blacklozenge . (craze-generating stress: 24.4 MPa, breaking stress: 50.0 MPa).

Table IV. Normalized Stress at the Tip of the Edge vs. Processing Angle

Processing angle ($^\circ$)	Stress (tip of the edge) (MPa)	Processing stress (MPa)
90	8.03	5.68
100	8.03	6.25
110	8.03	7.00
125	8.03	8.70
140	8.03	11.74

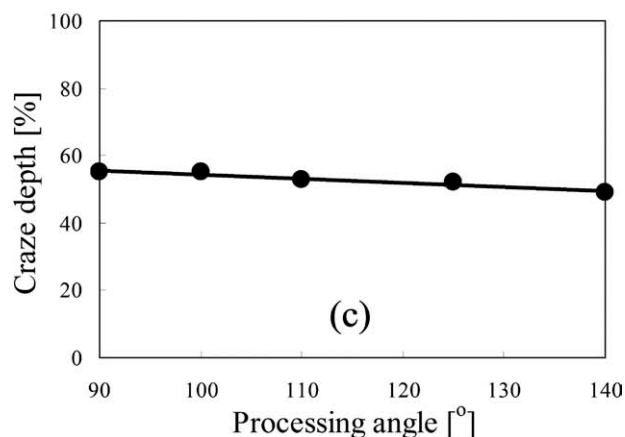
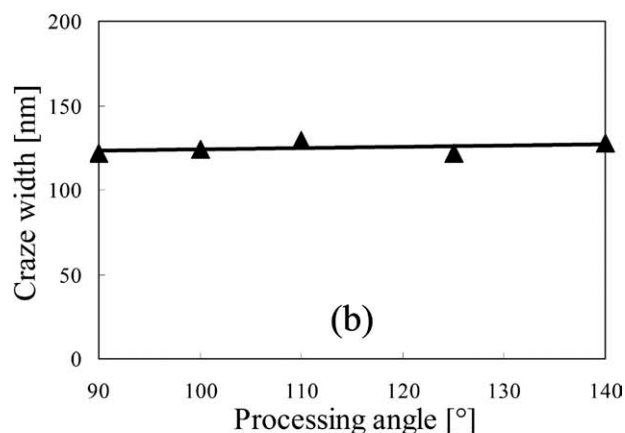
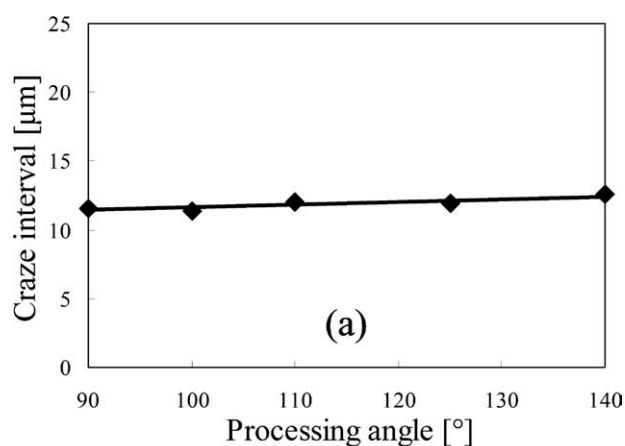


Figure 11. (a) Craze interval, (b) craze width, and (c) craze depth vs. the processing angle of periodically crazed PMMA films (processing stress: 7 MPa, processing rate: 10 mm/min).

processing stress are determined according to the procedure described above. These relationships are summarized in Table III.

Figure 9 shows a plot of maximum stress vs. craze depth for hypotheses 1 and 2. In Figure 10, the processing stress vs. craze depth plot of Figure 9 has been converted into processing stress vs. maximum stress. In the case of hypothesis 1, even if the processing stress is zero, a maximum stress of 37 MPa is applied by the edge. The maximum stress increases linearly with the processing stress. The curvature radius of the edge measured using the optical microscope was about 90 μm , whereas its calculated value was 527 μm . These results suggested that the film does not bend along the shape of the tip of the edge. In hypothesis 2, the increase in the maximum stress is not linear with respect to the processing stress. The variation in the maximum stress decreases as the processing stress increases.

In the experimental results, the craze interval increases and the craze width decreases as the processing stress increases. Their respective variations decrease as the processing stress increases. This observation is similar to the trend obtained for the processing stress vs. maximum stress curve that follows hypothesis 2. This tendency of craze interval can be explained by the time difference between the initial stress concentration and the instant of stress release, which decreased as the stress increased. Therefore, the craze is induced as a result of a three-point bending applied by the tip of the edge. The film bends according to the curvature induced by the three-point bending, and thus stress generated. In the next section, the validity of this hypothesis is verified by a simplified three-point bending model where the stress applied to the tip of the edge is standardized.

Standardization of the Stress Applied to Tip of the Edge

The tension applied to the film was resolved into vertical and horizontal components as shown in Figure 8(a,b). In this experiment, the processing stress is given by the setting for which the stress applied to the tip of the edge (horizontal element of the tension/sectional area) remains constant even if the processing angle is varied. The relationship between the processing angle and the stress applied to the tip of the edge is summarized in Table IV. The processing angle dependence on the craze interval, the craze width, and the craze depth is shown in Figure 11. The craze interval, the craze width, and the craze depth remained constant for all processing angles. Therefore, hypothesis 2 is more plausible than hypothesis 1.

CONCLUSION

In this article, it was determined that periodic crazing is induced by a three-point bending at the tip of the edge. Thus, a film is bent with a curvature determined by the three-point

bending, which applies a stress. As a result, crazing is induced. The amount of stress applied to the film when the craze formed was also studied. It is possible to directly determine the values of parameters such as craze depth, etc., from the physical material properties and the processing conditions of the sample if the complex shape of the bending owing to the tip of the edge is defined in advance. If the latter is possible, and the periodic craze can be controlled more precisely, there is a possibility such that periodically crazed films may be used as polarizing films.

ACKNOWLEDGMENTS

This research was supported by the Ministry of Education, Culture, Sports, Science and Technology and the Region Innovation Cluster Program (Tokai Region Knowledge Cluster Initiative).

REFERENCES

1. Sha, Y.; Hui, C. Y.; Ruina, A.; Kramer, E. J. *Acta Mater* **1997**, *45*, 3555.
2. Sun, B. N.; Hou, H. S.; Hsiao, C. C. *Eng. Fract. Mech.* **1988**, *30*, 595.
3. Tijssens, M. G. A.; van der Giessen, E.; Sluys, L. J. *Int. J. Solids Struct.* **2000**, *37*, 7307.
4. Tijssens, M. G. A.; van der Giessen, E.; Sluys, L. J. *Mech. Mater.* **2000**, *32*, 19.
5. Basu, S.; Mahajan, D. K.; van der Giessen, E. *Polymer* **2005**, *46*, 7504.
6. De Focatiis, D. S. A.; Buckley, C. P. *Polym. Test* **2008**, *27*, 136.
7. Takeno, A.; Miwa, M. Jpn. Pat. 3,156,058(1994).
8. Takeno, A.; Furuse, Y.; Miwa, M. *Adv. Comp. Mater.* **1994**, *4*, 129.
9. Takeno, A.; Yoshimura, M.; Miwa, M.; Yokoi, T. *Sen'i Gakkaishi* **2001**, *57*, 301.
10. Takeno, A. *Sen'i Gakkaishi* **2008**, *64*, 432.
11. Marissen, R. *Polymer* **2000**, *41*, 1119.
12. Luo, W.; Liu, W. *Polym. Test* **2007**, *26*, 413.
13. Volkov, A. V.; Tunyah, A. A.; Moskvina, M. A.; Dement'ev, A. I.; Yaryshev, N. G.; Volynskii, A. L.; Bakeev, N. F. *Polym. Sci. Ser. A* **2011**, *53*, 158.
14. Takeno, A.; Nakagaki, N.; Miwa, M. *Adv. Comp. Mater.* **1998**, *7*, 35.
15. Schirrer, R. *Polymer* **1988**, *29*, 1615.
16. Wu, S. *Polym. Eng. Sci.* **1990**, *30*, 753.
17. Wu, S. *Polym. Eng. Sci.* **1992**, *32*, 823.